LANGMUIR

Interfaces: Adsorption, Reactions, Films, Forces, Measurement Techniques, Charge Transfer, Electrochemistry, Electrocatalysis, Energy Production and Storage

Aldehyde-mediated protein-to-surface tethering via controlled diazonium electrode functionalization using protected hydroxylamines

Nicholas David James Yates, Mark R Dowsett, Phillip Bentley, Jack A Dickenson-Fogg, Andrew Pratt, Christopher Francis Blanford, Martin Fascione, and Alison Parkin

Langmuir, **Just Accepted Manuscript** • DOI: 10.1021/acs.langmuir.9b01254 • Publication Date (Web): 13 Nov 2019

Aldehyde-mediated protein-to-surface tethering via controlled diazonium electrode functionalization using protected hydroxylamines

Nicholas D. Yates,[1] Mark R. Dowsett,[1] Phillip Bentley,[2] Jack A. Dickenson-Fogg,[1] Andrew Pratt,[2] Christopher F. Blanford,[3] Martin A. Fascione,[1,] and Alison Parkin[1,]**

1. Department of Chemistry, University of York, Heslington, York, YO10 5DD, United Kingdom

2. Department of Physics, University of York, Heslington, York, YO10 5DD, United Kingdom

3. School of Materials, University of Manchester, Oxford Road, Manchester, M13 9PL, United Kingdom

4. Manchester Institute of Biotechnology, University of Manchester, 131 Princess Street, Manchester, M1 7DN, United Kingdom

*E-mail martin.fascione@york.ac.uk, alison.parkin@york.ac.uk.

ABSTRACT. We report a diazonium electro-grafting method for the covalent modification of conducting surfaces with aldehyde-reactive hydroxylamine functionalities that facilitate the wiring of redox-active (bio)molecules to electrode surfaces. Hydroxylamine near-monolayer formation is achieved via a phthalimide-protection and hydrazine-deprotection strategy that overcomes the multilayer formation that typically complicates diazonium surface modification. This surface modification strategy is characterized using electrochemistry (electrochemical impedance spectroscopy and cyclic voltammetry), X-ray photoelectron spectroscopy and quartz crystal microbalance with dissipation monitoring. Thus-modified glassy carbon, boron-doped diamond and gold surfaces are all shown to ligate to small molecule aldehydes, yielding surface coverages of 150-170, 40 and 100 pmol cm^{-2}, respectively. Bio-conjugation is demonstrated via the coupling of a dilute (50 μM) solution of periodate-oxidized horseradish peroxidase enzyme to a functionalized gold surface under bio-compatible conditions (H_2O solvent, pH 4.5, 25 °C).

INTRODUCTION

There is an ever-growing chemical biology toolkit of methodologies for site-selective bio-orthogonal ligations to proteins, meaning covalent bond formation reactions that target functionalities which are orthogonal to those which occur in Nature.[1-3] However, a relatively small number of these methodologies have been converted into robust strategies for immobilizing proteins onto a wide range of solid substrates.[4-5] This is despite the need for protein immobilization in industrial biocatalysis, medical diagnostics, tissue culturing, environmental sensing and biophysical characterisation.[5-7] By developing a procedure that enables the functionalization of a wide range of solid substrates with near-monolayers of hydroxylamine, we enable the tethering of

aldehyde-containing (bio)molecules to solid-substrates via oxime bond formation. We illustrate the utility of this method with the immobilization of an aldehyde-functionalized horseradish peroxidase on a hydroxylamine-modified gold electrode surface. The redox-activity of this enzyme[8-9] enables us to detect its presence on gold surfaces via electrochemistry, while quartz crystal microbalance with dissipation monitoring probes the change in mass of the electrode surface throughout the deprotection and protein-coupling process.

Scheme 1. The ligation of a hydroxylamine to an aldehyde or ketone to form an oxime.

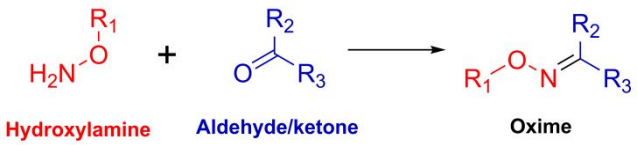

An oxime bond is formed via reaction between an organic hydroxylamine and an aldehyde or a ketone (Scheme 1).[10] It is such a robust and reliable reaction that it has been described as "Click" chemistry.[11] In the protein-immobilization strategy described here, we introduce a hydroxylamine group onto the solid substrate and react this with a protein aldehyde. It is advantageous to design a protein-immobilization strategy that targets aldehydes because there are a wide range of robust methodologies which will introduce these bio-orthogonal carbonyl functionalities into proteins, as shown in Figure 1.[10, 12-14]

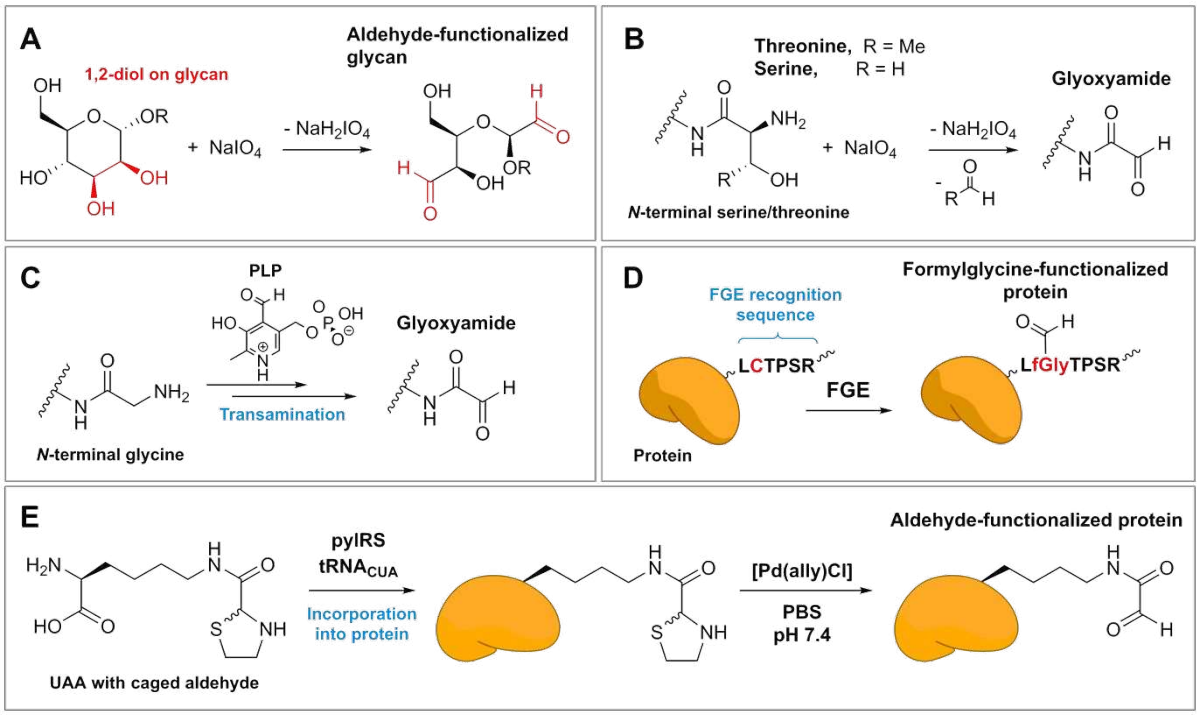

Figure 1. Summary of the variety of methods via which aldehyde motifs can be introduced into protein structures. (A) The oxidation of a glycan presenting a cis-1,2 diol with sodium periodate. (B) The oxidation of a 1,2-amino alcohol, such as *N*-terminal serine or threonine residues, with sodium periodate. (C) Pyridoxal 5'-phosphate (PLP) mediated transamination of *N*-terminal glycine residues. (D) Post-translational modification of a pre-installed recognition sequence by a formyl glycine generating enzyme. (E) Unnatural amino acid installation and manipulation.

In the case of glycoproteins, the chemical oxidation of glycans with sodium periodate is a simple way to generate aldehydes (Figure 1A).[10, 15] This is exemplified (*vide infra*) through the use of horseradish peroxidase, a redox-active heme-containing enzyme which presents glycan moieties that can be oxidized to bear aldehydes.[16-18] Proteins that are recombinantly produced in *E. coli* lack such glycosylation, instead they can be site-selectively modified to contain an aldehyde residue by a diverse range of methods including oxidation of an appropriate *N*-terminal amino acid residue

(Figure 1B and C),[10, 14] *in vivo* or *in vitro* post-translational modification of a pre-installed recognition sequence by a formylglycine generating enzyme (Figure 1D),[10, 12, 14] or unnatural amino acid installation (Figure 1E).[13, 19]

Prior to forming an oxime bond between a surface and a protein aldehyde, the solid substrate must first be decorated with hydroxylamine functionalities. This has previously been performed using long polymeric linkers on silicon.[20] However, the surface modification chemistry is not applicable to a broad substrate scope. Gold surfaces have also been functionalized via the formation of self-assembled monolayers using alkanethiol molecules capped with hydroxylamine groups.[21] Such a method cannot be translated to the multitude of different solid-materials which do not form stable surface-thiol bonds,[5] and gold-thiol bonds are not stable with respect to the application of potentials more negative than -0.9 vs SHE,[22] meaning such surfaces cannot be utilized in enzyme-catalyzed biofuel-production applications.[5] In contrast, the reduction of aryl diazonium salts is a widely adopted strategy for introducing chemical functional groups onto surfaces.[23-24] Indeed, diazonium modification has even been used for protein-surface attachment, although only via non-oxime ligation strategies.[25-28] The broad utility of diazonium surface-modification originates from the fact it generates a stable carbon-to-surface covalent bond on a large variety of different substrates, ranging from semi-conductors (e.g. silicon,[23-24] boron-doped diamond (BDD)),[29] to metals (e.g. gold),[23-24] other metallic conductors (e.g. graphite),[23-24] and dielectrics[23-24] (Scheme 2).

Scheme 2. The grafting of thick organic multilayers onto electrode surfaces via the reduction of diazonium cations.

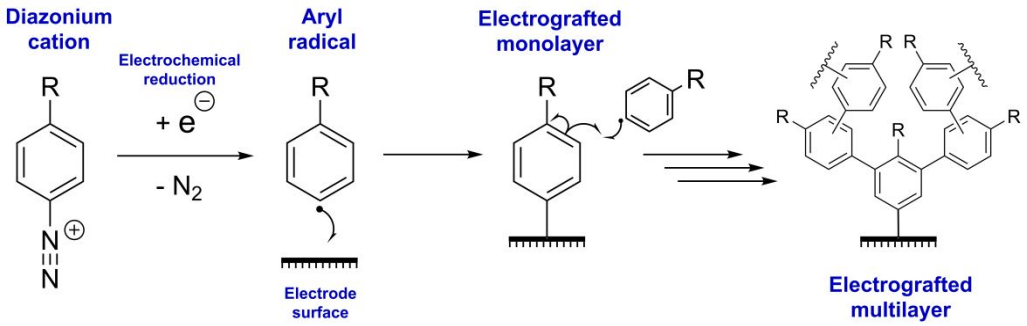

The limitation of the diazonium surface-modification methodology is that multilayer formation often results, as illustrated in Scheme 2.[23-24, 30-31] The nm-scale thickness often associated with such multilayers[32] is too large to support rapid electron transfer to redox active proteins and enzymes anchored onto the surface.[33] Methodologies to achieve a monolayer surface coverages from diazonium electro-grafting have been developed that are based on using sterically hindered aryl diazonium motifs,[34-35] radical scavengers,[36] and the application of short chronoamperometric pulses.[37-38] However, here we utilize a phthalimide-deprotection approach that enables electrochemical functionalization of a variety of surfaces with a near-monolayer of hydroxylamine functionalities, as summarized in Scheme 3. The inspiration for this approach originates from the works of Hauquier[39] and Downard[40] et al, who reported the introduction of amine functionalities onto glassy carbon[39-40] and gold[39] electrodes via the immobilization of a diazonium molecule bearing a π-containing protecting group on the amine moiety.[39-40] The aromatic protecting groups serve as a sacrificial shield that reacts with the excess radicals generated in the diazonium reduction reaction. The subsequent removal of the protecting groups thus strips the electrode of much the thick, inhomogeneous multilayer,[39-40] with Downard using atomic force microscopy (AFM) to prove monolayer formation.[40] This broader concept of protection-deprotection diazonium electro-grafting has also been applied to functionalize surfaces with aldehydes,[41] thiols,[42] and alkynes,[43] although AFM often indicates near-monolayer, rather than strict monolayer, surface modification. We demonstrate that phthalimide-protection/deprotection can be used to yield a near-monolayer

of hydroxylamine-surface functionality. We present the use of a stable triazene precursor which enables generation of diazonium molecules *in situ*[44-46] and makes our methodology amenable to benchtop reaction conditions (Scheme 3). We prove the presence of hydroxylamine groups on the surface using electrochemical and surface analysis techniques.

Scheme 3. Summary of the surface modification strategy and aldehyde ligation experiments described in the paper.

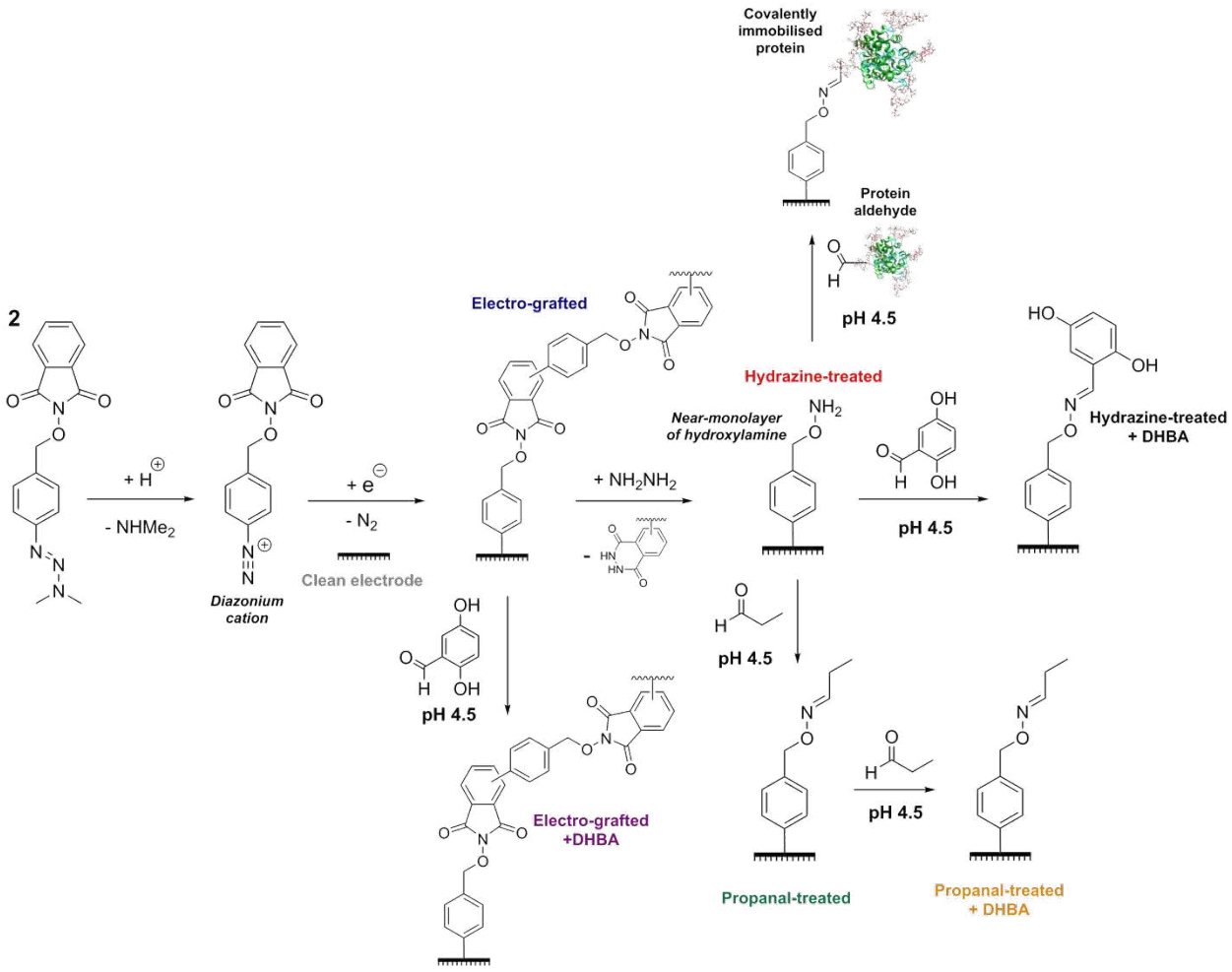

We illustrate the broad utility of this new surface-modification methodology by showing the functionalization of glassy carbon, gold and boron doped diamond surfaces, and prove that our hydroxylamine-functionalized surfaces have a high affinity for small molecule aldehydes (Scheme 3). We demonstrate that bioconjugation of an aldehyde-functionalized protein can be performed

under biocompatible conditions via the generation of a horseradish peroxidase functionalized gold electrode.

EXPERIMENTAL SECTION

Synthesis. The synthesis methodology used to generate (E)-(4-(3,3-dimethyltriaz-1-en-1-yl)phenyl)methanol, designated **1**, Scheme S1, and (E)-2-((4-(3,3-dimethyltriaz-1-en-1-yl)benzyl)oxy)isoindoline-1,3-dione, designated **2** and shown in Scheme 3, is described in the SI where details of all characterisation methods and data (NMR, (ESI)HRMS and FT-IR) is also presented (Figure S1-S8).

Electrochemical set-up. Electrochemical experiments were conducted in a water-jacketed all-glass electrochemical cell capable of supporting a three-electrode setup (constructed in-house). A thermostated water-circulator (Grant) was used to maintain temperature control. The disk working electrodes (3 mm diameter) used in the cyclic voltammetry and EIS electrochemical surface-analysis experiments were either purchased from eDAQ (glassy carbon and gold electrodes) or Windsor Scientific (boron-doped diamond electrodes). The Pt wire counter electrode was made in-house from wire of 1 mm diameter purchased from Sigma-Aldrich. The Ag/AgCl/3.0 M sodium chloride reference electrode was from eDAQ. All potentials have been converted to versus the standard hydrogen electrode using the correction factor of E (V vs SHE) = E (V vs Ref) + 0.205, which was experimentally determined using the ferricyanide redox couple as calibration.[47] The potentials reported for the experiments performed in 1:5 v:v water:acetonitrile + 0.1 M tetrabutylammonium hexafluorophosphate (Bu_4NPF_6) electrolyte do not account for any junction potential that may exist between the Ag/AgCl/3.0 M sodium chloride reference electrode and the mixed solvent electrolyte. All experiments that were conducted under a nitrogen atmosphere were

carried out in a nitrogen-filled glovebox of dioxygen ≤ 40 ppm, otherwise experiments were performed in air.

An EmStat^3 potentiostat (PalmSens) with PSTrace 5.5 for Windows software was used for the diazonium electro-grafting experiments. The electrochemical assays of surface confined quinone species were conducted using a CompactStat potentiostat (Ivium technologies) with IviumSoft software for Windows. The electrochemical impedance spectroscopy experiments were carried out using a Plamsens4 potentiostat and details of the data analysis are provided in the SI (Figure S9).

Hydroxylamine-functionalization of the disk electrodes. The disk electrodes were cleaned using the following procedures. Glassy carbon electrode surfaces were mechanically polished for 1-2 min using 1-5 μm alumina slurry impregnated onto a *WhiteFelt* polishing pad (Buehler). Electrodes were then rinsed with milliQ water and sonicated in acetonitrile for 5 min. Gold electrodes were polished for approximately 1 min using nylon polishing pads (Buehler) impregnated with 1 μm RS PRO Blue Diamond Paste (RS Components Ltd) and then for approximately 1 min with a 1/10 μm RS PRO Grey Diamond Paste (RS Components Ltd). This was followed by polishing for approximately 1 min using 1-5 μm alumina slurry impregnated onto a *WhiteFelt* polishing pad, then rinsing and sonication for 1 min in milliQ water. Electrochemical polishing was then performed by recording 50 cyclic voltammograms from 0.35 to 1.81 V vs SHE in 0.5 M H_2SO_4 at 100 mV s^{-1}, after which the electrodes were rinsed with milliQ water and immersed in in milliQ water until used. Boron doped diamond electrodes were polished for 1-2 min using nylon polishing pads (Buehler) impregnated with 1 μm RS PRO Blue Diamond Paste (RS Components Ltd) and for approximately 1 min using a 1/10 μm RS PRO Grey Diamond Paste (RS Components Ltd). The electrodes were then rinsed with milliQ water and sonicated in acetonitrile for 5 min.

Once the disk electrodes were cleaned, they were hydroxylamine-functionalized using the following procedure for *in situ* diazonium cation generation and electro-grafting, and subsequent hydrazine deprotection. 2 μL of a 6.6 M hydrochloric acid solution was added to 100 μL of a 15 mM solution of **2** in a 1:5 v:v water:acetonitrile + 0.1 M Bu_4NPF_6 solvent system at 0 °C, triggering the formation of diazonium cations via protonation of the triazene moiety.[44] 65 μL of this solution was added to 935 μL of 1:5 v:v water:acetonitrile + 0.1 M Bu_4NPF_6 at 0 °C yielding a solution of a 1 mM maximum diazonium salt concentration. Electrochemical grafting experiments to yield an electro-grafted surface (Scheme 3) were carried out by cycling between the potentials shown in the relevant figures at a scan rate of 20 mV s^{-1} and 0 °C. After electrochemical grafting, the electrode surfaces were cleaned by sonication in acetonitrile for 2 min and then rinsed with milliQ water before being allowed to dry in air. The hydrazine deprotection step (Scheme 3) was carried out by adding 155 μL of hydrazine monohydrate to 2 mL ethanol and heating the resultant solution to 80 °C. The grafted electrodes were then placed into this solution for either 5 min (glassy carbon and boron-doped diamond electrodes) or 10 min (gold) with the intention of yielding the hydroxylamine near-monolayer "hydrazine-treated" surface depicted in Scheme 3. The electrodes were then allowed to cool for 30 s in a 10 μM ice-cold solution of (aminooxy)acetic acid hemihydrochloride, a solution designed to prevent cross-contamination of the hydroxylamine surfaces with trace carbonyl species. Prior to treatment of the surfaces with target aldehyde species the electrodes were rinsed briefly in ice-cold water and dried under a stream of argon.

Reaction of hydroxylamine-functionalized disk electrodes with aldehyde-containing species. To investigate propanal binding to hydroxylamine-functionalized glassy carbon surfaces modified disk electrodes were placed in aqueous pH 4.5 buffer solution (100 mM sodium acetate + 150 mM sodium chloride) spiked with 5 % v/v propanal for 1 hour at room temperature, after

which time the electrodes were rinsed with milliQ water and air-dried before electrochemical testing, *vide infra*.

To investigate 2,5-dihydroxybenzaldehyde binding to hydroxylamine-functionalized glassy carbon, boron-doped diamond and gold disk electrodes thus-modified disk electrodes were placed in a 50 μM solution of 2,5-dihydroxybenzaldehyde in aqueous pH 4.5 buffer solution (100 mM sodium acetate + 150 mM sodium chloride). The reaction was left overnight at room temperature, after which time the electrodes were rinsed with milliQ water and sonicated with acetonitrile for 30 s prior to cyclic voltammetric interrogation at 25 °C in aqueous pH 4.0 buffer solution (100 mM sodium acetate + 150 mM sodium sulfate).

Oxidized horseradish peroxidase surface-immobilization. Oxidized horseradish peroxidase (EZ-Link™ Plus Activated Peroxidase) was purchased from Thermo Scientific. For the electrode-protein ligation experiment, hydroxylamine-functionalized 3 mm gold disk electrodes were treated with a 50 μM solution of oxidized horseradish peroxidase in aqueous pH 4.5 buffer solution (100 mM sodium acetate + 150 mM sodium chloride). The reaction was left to proceed overnight at room temperature, after which time the electrodes were rinsed with aqueous pH 7.4 100 mM sodium phosphate buffer solution prior to electrochemical analysis. Control experiments were performed by carrying out the same procedure but using non-oxidized, native horseradish peroxidase (peroxidase from horseradish, Type I, Sigma-Aldrich). The concentration of the horseradish peroxidase solutions was determined using the extinction coefficient $\varepsilon = 100$ mM cm^{-1} at 403 nm.[48]

Solution-phase analogues of surface chemistry reactions. As detailed in the SI, solution-phase experiments were carried out to probe the surface-phase chemistry. Figures S14-25 show

the NMR, (ESI)HRMS and FT-IR data of the products isolated from hydrazine deprotection of **2** to yield (E)-O-(4-(3,3-dimethyltriaz-1-en-1-yl)benzyl)hydroxylamine, designated as **3** (Scheme S3); oxime reaction of **3** with 2,5-dihydroxybenzaldehyde; and reaction of o-benzylhydroxylamine with 2,5-dihydroxybenzaldehyde.

X-ray photoelectron spectroscopy. The X-ray photoelectron spectroscopy (XPS) experiments were conducted using a monochromated Al Kα source at 1486.6 eV (XM1000, Scienta Omicron GmbH) in an ultrahigh vacuum system with a base pressure below 2×10^{-10} mbar. X-rays were incident at 22.5° to the sample normal and at 45° to the hemispherical energy analyzer (EA 125, Scienta Omicron GmbH) used to detect emitted photoelectrons. An input aperture diameter of 6 mm was used for all scans.

To prepare the samples for XPS analysis, gold-coated silicon wafer (99.999% (Au), layer thickness 1000 Å, 99.99% (Ti adhesion layer)) was purchased from Sigma-Aldrich and cut into 8 mm × 8 mm squares. A solution of acidic piranha (caution: highly corrosive) was prepared by adding 1 part of 30% hydrogen peroxide to 3 parts of concentrated sulfuric acid. The solution was used while hot to clean the 8 mm × 8 mm samples, which were only removed after reaction had ceased. The gold substrates were then rinsed with water and dried under a stream of argon prior to electrochemical grafting (Figure S28). Any subsequent hydrazine-treatment was carried out as described for disk electrodes.

Survey scans on the three surfaces tested were measured from a binding energy of 700 eV to 0 eV in -0.3 eV steps and a with dwell time of 0.5 s. To allow comparison of relevant peaks, these scans were normalized to the average count measured between 600 and 700 eV. High resolution core level spectra were measured over the range of the O 1*s*, N 1*s* and C 1*s* peaks of interest with

-0.05 eV steps and a 1 s dwell time; typically, five separate scans were obtained, then averaged. For the O 1*s* and C 1*s* peaks the data were normalized to the relative weights observed in the survey spectra. The N 1*s* data were scaled to give a consistent noise level.

Quartz crystal microbalance with dissipation monitoring. A Qsense E1 quartz crystal microbalance with dissipation monitoring (QCM-D) was used to quantify mass changes associated with the deprotection of the grafted layer and subsequent protein coupling. A QSX301 quartz crystal microbalance chip purchased from QSense (f_0 = (4.95 ± 0.05) MHz) was used as the solid substrate and cleaned with a solution of basic piranha that was prepared by adding 1 part of 30% hydrogen peroxide to 3 parts of ammonium hydroxide solution. The resultant solution was then heated to 60 °C and used for cleaning while hot. Once reaction between the piranha solution and the gold surface ceased, the gold chip was subjected to UV/ozone treatment prior to electrochemical grafting. Cyclic voltammograms of the electro-grafting procedure are shown in Figure S31. Post-grafting, the chip was rinsed in water and then ethanol. After loading into the QCM-D instrument, the electro-grafted surface was temperature-equilibrated with 50 °C ethanol in a custom-built open-topped static chamber attached to a standard QSense base. The frequency and dissipation responses from odd harmonics from 3 to 13 were probed in sequence with a time resolution of approximately 0.8 s. After thermal equilibrium was reached, hydrazine monohydrate was added such that an 7 % v/v solution of hydrazine in ethanol was obtained. After deprotection had been observed via an increase in Δf, the hydrazine ethanol solution was replaced with a solution of 1 μM hydrazine monohydrate in distilled water. This solution was then exchanged with aqueous pH 4.5 buffer solution (100 mM sodium acetate + 150 mM sodium chloride), then a 35 μM solution of horseradish peroxidase in the same buffer was added, and the response in Δf observed. Finally, the solution of horseradish peroxidase was exchanged for ethanol.

RESULTS AND DISCUSSION

Triazene **1** (Scheme S1 and Figures S1-4) was synthesized from commercially available 4-aminophenol (yield 73%), before derivatization to yield phthalimide-functionalized triazene **2** (yield 51%, Scheme 3 and Figures S5-8). Triazene **2** was designed to permit the functionalization of any conducting surface with a near-monolayer of hydroxylamine. The aryl triazene functional group has been previously used as an acid-labile protecting group for aryl diazonium species,[44-46] and the propensity of **2** to form diazonium species upon protonation is evidenced by the presence of a species of m/z 280.07 in the ESI-MS (Figure S7). The acid-triggered *in situ* generation of the diazonium species from triazene **2** and the subsequent reductive electro-grafting process on a glassy carbon electrode was followed using cyclic voltammetry (Figure 2). The broad reductive wave (negative current) that is observed as the potential of the electrode is decreased from approximately +0.6 to 0 V vs SHE in scan 1 is typical of diazonium reduction,[23-24, 49] and the disappearance of this feature in subsequent scans indicates the formation of a thick multilayer.[39, 50]

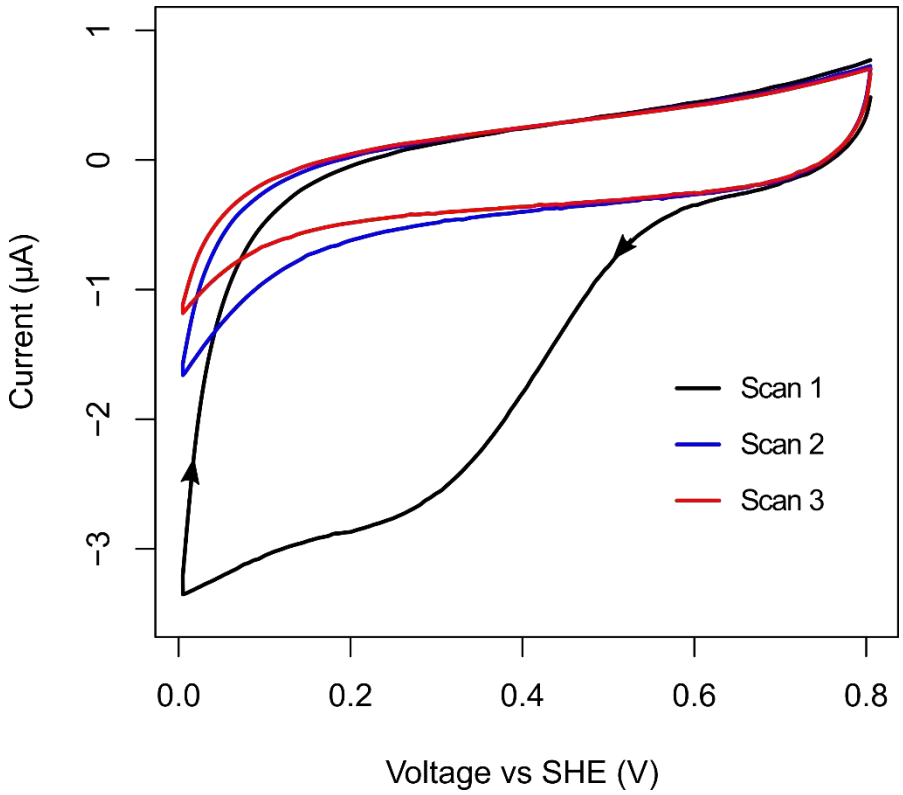

Figure 2. Cyclic voltammograms of a glassy carbon electrode during 20 mV s^{-1} electroreductive modification scans with the aryl diazonium salt generated *in situ* from **2** in 1:5 v:v water:acetonitrile and 0.1 M Bu_4NPF_6, 0 °C. The scans commence at the most positive potential, then the voltage is lowered before being increased again. Arrowheads on black scans differentiate between the oxidative and reductive sweeps.

As reported by Hauquier,[39] the treatment of electro-grafted electrode surfaces with a solution of hydrazine monohydrate in ethanol at 80 °C serves to remove phthalimide protecting groups, stripping the multilayer from the electrode surface, see Scheme 3. For our hydroxylamine system, the hydrazine also serves a secondary function, acting as a scavenger for trace carbonyl species

and thus preventing the reaction of the modified surface with contaminant carbonyl compounds such as ethanal or acetone.

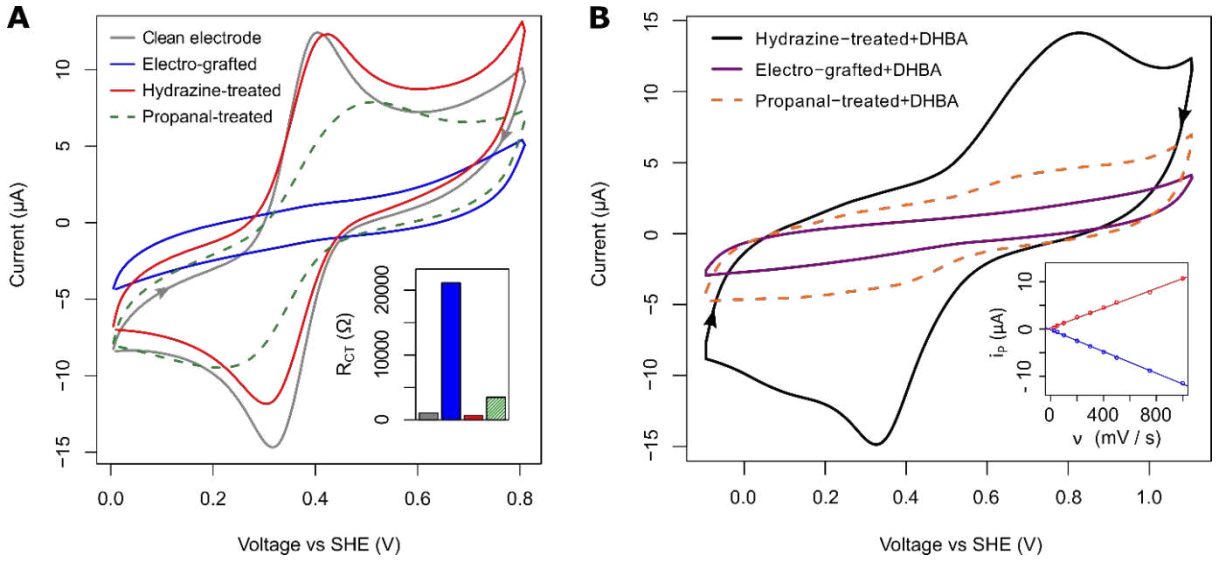

Figure 3. (A) Cyclic voltammograms of glassy carbon electrodes from various stages in the modification process and after a "quench" reaction with propanal, all scans were measured at 500 mV s^{-1} in an aqueous solution of 1 mM ferricyanide and 0.1 M sodium chloride. (A, inset) The change in the resistance to charge transfer (R_{CT}) determined from EIS experiments measured on the same electrodes and under the same experimental conditions. (B) Cyclic voltammograms of glassy carbon electrodes from various stages in the modification process and after a "quench" reaction with propanal that have been subsequently reacted with 2,5-dihydroxybenzaldehyde (DHBA). All scans were measured at 500 mV s^{-1}, nitrogen, in aqueous pH 4.0 buffer solution (100 mM sodium acetate + 150 mM sodium sulfate). (C, inset) Analysis of the quinone-derived baseline-subtracted anodic (red) and cathodic (blue) peak currents shows a linear relationship to scan rate (ν). In panels A and B the arrowheads differentiate between the oxidative and reductive sweeps.

As shown in Figure 3A, the glassy carbon electrode modification process can be monitored via cyclic voltammetry in aqueous ferricyanide solutions. Unmodified glassy carbon electrodes show the expected solution-voltammetry responses for reversible ferricyanide electrochemistry,[50] while electrode surfaces which have been subjected to electro-grafting (Scheme 3) display only a non-Faradaic (capacitive-only) voltammetric response to the same solution. Glassy carbon electrodes which have been electro-grafted and subsequently treated with hydrazine show a return to the typical solution-voltammetry response. The inhibition of the redox chemistry upon electro-grafting is attributed to the formation of a thick multilayer that is impermeable to the ferricyanide. The fact that hydrazine-treatment restores the reversible solution voltammetry indicates that deprotection of the phthalimide moiety strips the impermeable multilayer from the surface of the electrode.

Electrochemical impedance spectroscopy (EIS, Figure S9) can also be carried out on different electrode surfaces in a solution of ferricyanide. As shown in Figure 3A, the changes to the resistance to charge transfer (R_{CT}) values extracted from analysis of this data provide further evidence that the electro-grafting and hydrazine-treatment processes have a profound effect on the surface chemistry of a glassy carbon electrode. The high R_{CT} value of the electro-grafted surface is consistent with the notion that diazonium-modification forms an electrically insulated multilayer on the surface of the electrode.

Evidence that electro-grafting followed by hydrazine-treatment generates a hydroxylamine functionalized surface is provided by reacting a thus-modified glassy carbon electrode with propanal. Propanal is a simple aldehyde which would be expected to undergo facile ligation to a hydroxylamine-modified surface, generating a neutral oxime species. This can be detected in the

EIS measurements in ferricyanide solution, with an increase in R_{CT} following propanal reaction of a hydrazine-treated electrode (Figure 3A; Table S1 and Figure S10). Voltammograms measured in the same ferricyanide solution also highlight that the surface chemistry of the electrode has changed following reaction with propanal. The drop in peak current and increase in the peak-to-peak voltage separation is consistent with the generation of a passivated electrode surface.

It is possible to estimate the coverage of hydroxylamine functionalities on the hydrazine-treated electrode surfaces via oxime ligation to the redox active species 2,5-dihydroxybenzaldehyde. This generates an electrode that shows surface-bound quinone redox chemistry (Figure 3B and Scheme S2) that is comparable to data in the literature for surface-confined quinones.[51-53] Specifically, the broad nature of the oxidative peak and the shoulder present in the reductive peak result from the complicated square scheme that describes the variety of proton-coupled electron-transfer pathways via which the two-electron quinone redox chemistry can proceed.[53] The large separation in the potentials of peak oxidative and reductive current is expected based on literature data on surface-confined quinone species.[51-53] The potential window of the redox process also correlates with published data[51-53] and solution-phase voltammetry of 2,5-dihydroxybenzaldehyde recorded under the same conditions as the data in Figure 3 (see Figure S12).

The peak-current response scales linearly with scan rate in a manner that is indicative of surface confinement (Figure 3B and Figure S11).[40, 51-54] The electroactive coverage of the redox active quinone units, calculated via integration of the baseline-subtracted cathodic peaks,[54] was found to be 150-170 pmol cm^{-2} (Equation S1). This compares well to a theoretical maximum surface coverage of 182 pmol cm^{-2}, calculated by approximating that each electrode-confined quinone-species is orientated perpendicular to the surface, occupies a circular surface area of 1.21×10^{-14} cm^2 (based on a molecular diameter of 10.27 Å from Chem3D) and is hexagonally close-packed.

The experimental coverage data is also in good agreement with the 100-250 pmol cm^{-2} coverage of ferrocene units that has been reported when coupling activated ester ferrocene-derivatives to glassy carbon electrodes functionalized with monolayers of alkyl amine functionalities.[39]

Hydrazine-treated glassy carbon electrodes that have been reacted with propanal prior to exposure to 2,5-dihydroxybenzaldehyde fail to show surface-bound quinone redox chemistry, which is consistent with the hydroxylamine electrode-functionalities being unavailable for reaction with 2,5-dihydroxybenzaldehyde due to quenching via oxime ligation to propanal (Figure 3B). The reaction of hydrazine-treated electrodes with hydroquinone, rather than the aldehyde containing derivative 2,5-dihydroxybenzaldehyde, also fails to yield surface-confined quinone species (Figure S13). This shows that the presence of the aldehyde on 2,5-dihydroxybenzaldehyde is critical to the surface confinement of a quinone-containing molecule, and that surface-confined redox chemistry is not observed due to simple adsorption. The proclivity of 2,5-dihydroxybenzaldehyde towards oxime ligation with solution-phase hydroxylamine species has also been demonstrated (Scheme S3, Figures S14-S25).

To demonstrate that the hydroxylamine-surface functionalization methodology can be applied to a wide range of different conducting materials, boron-doped diamond and gold electrodes were modified using the same two-step diazonium electroreduction and subsequent deprotection strategy previously described for glassy carbon. As with glassy carbon, the diazonium electro-grafting process was monitored by cyclic voltammetry, see Figure 4. It is notable that both the onset potential and current changes with electrode material, an observation which is consistent with diazonium electrografting studies by other authors.[55-58] For both boron-doped diamond and gold, the substantial drop in reductive current which follows the first scan is again interpreted as evidence that a multilayer has formed on the electrode surface.

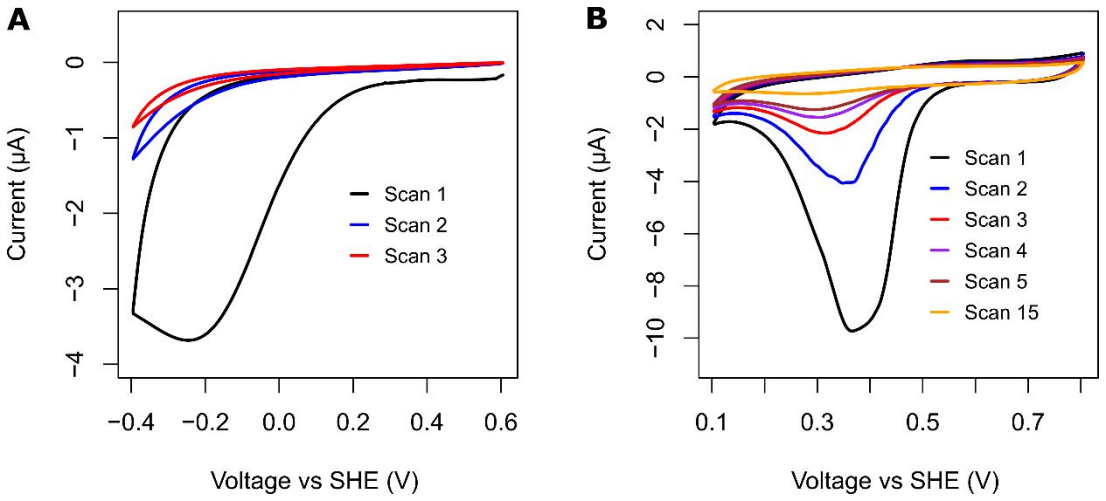

Figure 4. Cyclic voltammograms of (A) boron doped diamond and (B) gold electrodes during 20 mV s^{-1} electroreductive modification scans with the aryl diazonium salt generated *in situ* from **2** in 1:5 v:v water:acetonitrile and 0.1 M Bu_4NPF_6, 0 °C. The scans commence at the most positive potential, then the voltage is lowered to the most reductive potential before being increased again.

The reactivity of the boron-doped diamond and gold electrode surface-hydroxylamine groups with aldehyde species in solution is again probed using 2,5-dihydroxybenzaldehyde. Post-reaction, the presence of oxime-linked quinone-electrode species is detected in the cyclic voltammograms shown in Figure 5. As in the analogous glassy carbon experiments (Figure 3), the intensity of the peak current of the baseline-subtracted gold and boron doped diamond redox signals scales linearly with scan rate, as expected for a surface-confined quinone species (Figure 5, Figure S11).[40, 52, 54]

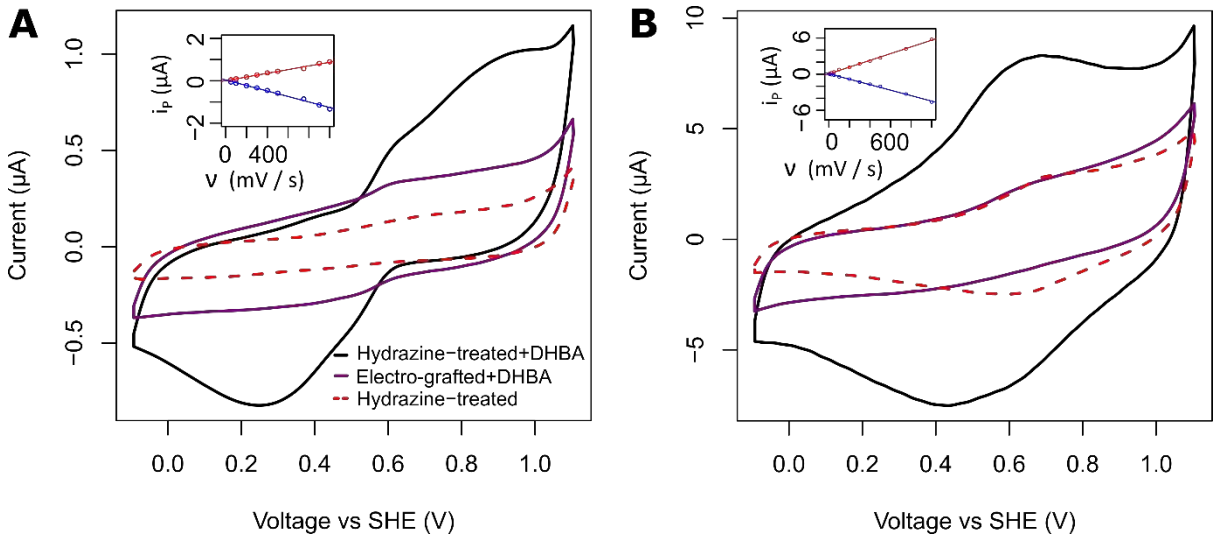

Figure 5. Cyclic voltammetry of (A) boron doped diamond electrode and (B) gold electrode which have been electro-grafted with compound **2**, and then (black line) hydrazine-treated prior to reaction with 2,5-dihydroxybenzaldehyde (DHBA), or (purple line) treated with DHBA while still in the electro-grafted state. (Red dashed line) Data from a control experiment where the hydrazine-treatment is not followed by DHBA reaction. (Insets) The magnitude of the baseline-subtracted (red) anodic and (blue) cathodic peak currents (i_P) vs scan rate (ν). The voltammograms shown were recorded at 500 mV s^{-1}, 25 °C, nitrogen, in an aqueous pH 4.0 buffer solution (100 mM sodium acetate + 150 mM sodium sulfate).

On the gold electrodes, a quinone surface-coverage of approximately 100 pmol cm^{-2} is derived. This value can be compared to the glassy carbon value of surface-coverage of approximately 160 pmol cm^{-2}. According to the literature, achieving a lower surface density modification on a gold electrode relative to glassy carbon is to be expected, with previous studies indicating that the coverage of ferrocene units which could be coupled to a gold surface functionalized with a

monolayer of alkyl amine functionalities was 5 to 12.5 times lower than that achieved using similarly functionalized glassy carbon electrodes.[39]

The surface modification of a gold electrode was further probed by using atomic force microscopy (AFM) to compare the surface morphology of gold that has been electro-grafted, hydrazine-treated and subsequently reacted with propanal with a gold surface control that was not diazonium-electrografted. As shown in Figure S26, the AFM imaging is consistent with the formation of a monolayer or a near-monolayer rather than a multilayer. Taking the electrochemical coverage data in context with the quinone coverage, we therefore conclude that the protection-deprotection methodology described yields glassy carbon and gold surfaces modified with a near-monolayer coverage of hydroxylamines.

Integration of the peak area of baseline-subtracted quinone signals quantifies the surface coverage of hydroxylamine moieties on boron doped diamond electrodes as approximately 40 pmol cm^{-2}. This value is reproducible in repeat experiments using different electrodes. This is a lower coverage than reported for ferrocene-coated boron-doped diamond electrodes generated via either Cu^{I}-catalysed click reaction between diazonium electro-grafted phenyl azide and ethynylferrocene (250 pmol cm^{-2});[59] or photochemical immobilization of vinylferrocene (450 pmol cm^{-2}).[60] Although these published modification strategies do not aim for struct monolayer coverage, and may therefore establish upper limit coverage ranges for boron doped diamond, it is notable that the quinone oxime-ligation coverage we measure on boron doped diamond is also far lower than the analogous glassy carbon measurement, a fact that is incongruent to the similarities in the electrografting voltammetry. Further experiments were therefore conducted to probe the impact of the hydrazine deprotection step on the surface chemistry of electro-grafted boron-doped diamond electrodes, using EIS and cyclic voltammetry measurements of $Fe(CN)_6^{3-/4-}$ in solution

(Table S1, Figure S10, Figure S27). Although the data is again consistent with the conclusion that hydrazine-treatment again strips a multilayer that results from the electro-grafting process, the drop in R_{CT} (6226 to 444.1 Ω) and changes in solution voltammetry are subtler than on glassy carbon. We therefore speculate that both a physisorbed and electro-grafted layer is deposited at BDD, and the physiosorbed groups are largely removed during cleaning. Improving the density of coverage on boron doped diamond will therefore need to be a key aim of future work.

The ability to modify gold, a metallic substrate, provides the opportunity to probe the derivatization state of the electrode surface via X-ray photoelectron spectroscopy (XPS). The standard voltammetric methodology for electro-grafting **2** onto surfaces was applied to two gold-coated silicon wafers that had been cleaned using acidic piranha solution (Figure S28), and one of these surfaces was subsequently hydrazine-treated. XPS measurements were then made of the two modified gold surfaces and a control, non-functionalized, piranha-cleaned gold surface. Evidence for multilayer formation on the electro-grafted surface is indicated by comparing the survey spectra data for this surface relative to that for the control clean unmodified gold surface; the carbon-to-gold and oxygen-to-gold peak ratios both increase for the modified surface relative to those for clean gold (Figure 6A).

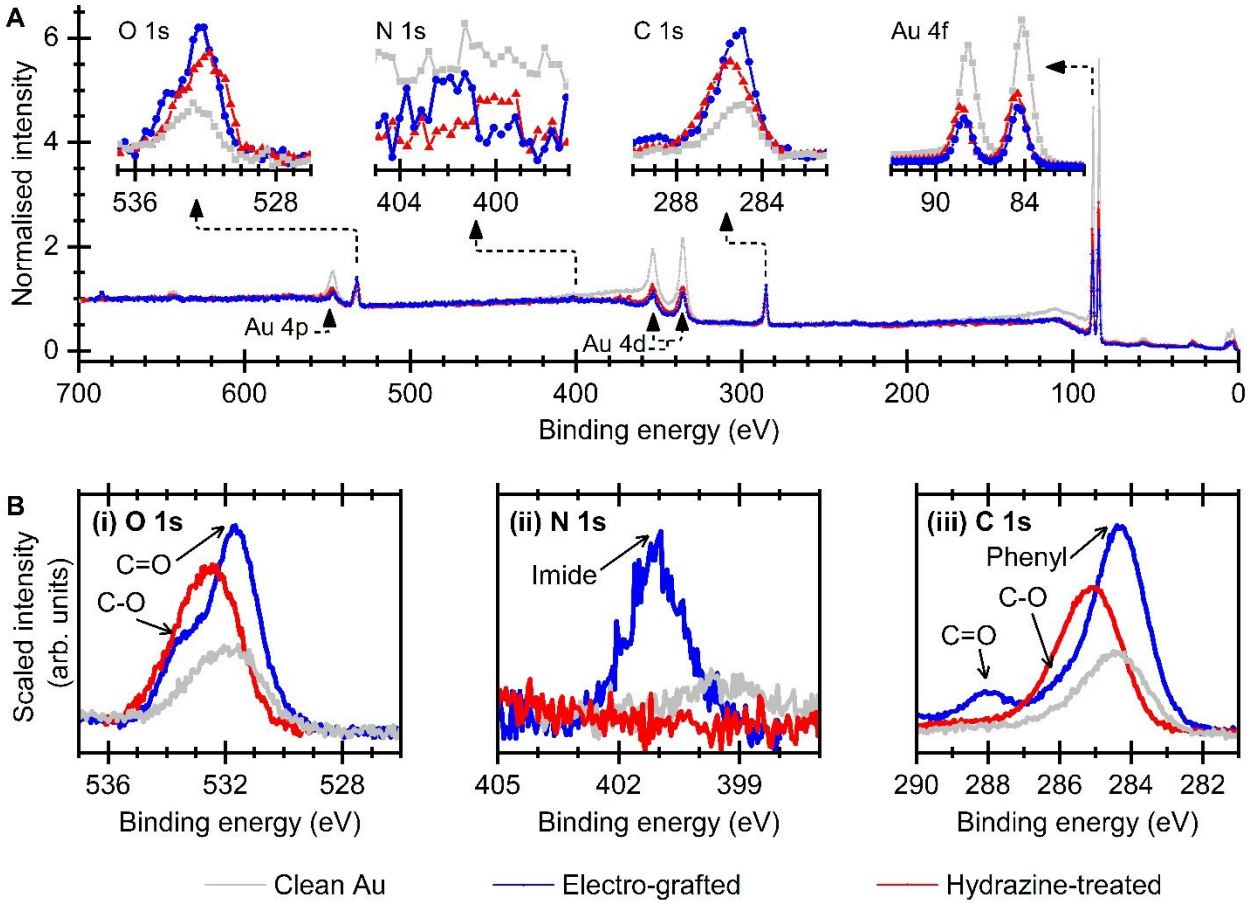

Figure 6. XPS of the surface of a gold-coated silicon wafer at different states of functionalization. (A) Survey scans, each with the intensity normalized to the average count between 600 and 700 eV. (B) Higher resolution scans of O 1*s*, N 1*s* and C 1*s* peaks. For (i) and (iii) the relative intensities were scaled using the survey scan data while for (ii) data is scaled to the noise level.

In detailed scans, the peak positions attributed to the different carbon and oxygen environments on the electro-grafted surface are expected based on the molecular structure of **2**,[61] with phenyl (~284.5 eV), C-O (~286.5 eV), and C=O (~288 eV) bonding features present in the C 1*s* spectra and C-O (531.5 eV) and C=O (533 eV) features in the O 1*s* spectra. The energy of the nitrogen

peak at ~401 eV is also consistent with that observed for imide-type nitrogen atoms (Figure 6B).[62] Thus, the XPS data supports the structure of the electro-grafting surface shown in Scheme 3. The notion that hydrazine deprotection of the phthalimide group strips a multilayer off electro-grafted gold surfaces is evidenced by the drop in the normalized intensity of the survey scan carbon and oxygen peaks following hydrazine-treatment, and loss of the phenyl signal (Figure 6A).

Horseradish peroxidase (HRP) is a highly glycosylated enzyme,[16-18] the glycans of which display many cis 1,2-diol sites that are converted into aldehydes via periodate oxidation (Figure 1A).[16-18] Gold electrodes in the hydrazine-treated, hydroxylamine-functionalized modification state were reacted with either oxidized (aldehyde-containing) horseradish peroxidase or native (aldehyde-free) horseradish peroxidase. We conclude that the aldehyde-containing horseradish peroxidase is ligated to the modified electrode via oxime bond formation because subsequent cyclic voltammetry (25 °C, nitrogen, pH 7.4) shows an intense reductive peak centered at approximately -0.15 V vs SHE and a broad oxidative peak centered around 0 V vs SHE (black line, Figure 7). The position of this signal correlates with that reported for other examples of immobilized horseradish peroxidase participating in direct-electron transfer with an underlying electrode surface and is attributed to the $Fe^{2+/3+}$ redox couple of the heme.[8-9]

Experiments using native horseradish peroxidase show that the faradaic current originating from heme redox chemistry is approximately 4-fold smaller for a hydroxylamine-coated gold electrode reacted with the aldehyde-free native horseradish peroxidase (grey line, Figure 7). This is consistent with the native enzyme being unable to partake in oxime ligation to the electrode surface, resulting in poorer electroactive coverage. Additional control experiments (Figure S29) further confirm our assignment of the faradaic signals to the redox activity of competent horseradish peroxidase immobilized on the electrode; this current is greatly diminished when

either boiled aldehyde-containing enzyme (i.e. natured protein and free heme) is applied to a hydrazine-treated electrode, or native (aldehyde-free) horseradish peroxidase is applied to bare gold, or when a hydrazine-treated electrode surface is incubated with an enzyme-free buffer solution (Figure S29).

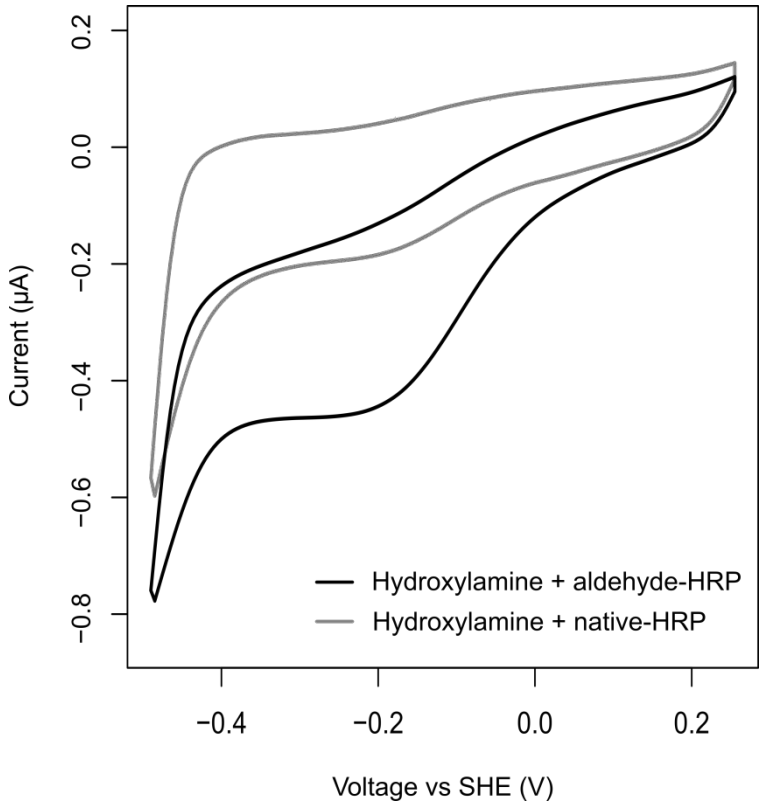

Figure 7. 30 mV s^{-1} cyclic voltammograms from when the oxidized, aldehyde-containing enzyme is reacted with a hydrazine-treated gold electrode (black line), and hydrazine-treated electrode surfaces are reacted with native (aldehyde-free) horseradish peroxidase (gray line). All experiments were conducted under nitrogen at 25 °C in pH 7.4 100 mM sodium phosphate buffer solution.

Enzyme-free experiments using hydrazine-treated, hydroxylamine-functionalized gold electrodes showed that these surfaces are highly effective at catalyzing the electroreduction of H_2O_2 (Figure S30). This precluded the chronoamperometric detection of the enzymatic activity of immobilized horseradish peroxidase. Further evidence for the immobilization of aldehyde-containing horseradish peroxidase onto hydrazine-treated gold electrode surfaces was instead obtained via quartz crystal microbalance with dissipation monitoring (QCM-D).

A gold-coated quartz crystal microbalance (QCM) sensor was electrochemically grafted with **2** (Figure S31) and washed successively in water and ethanol to remove any non-covalently attached organic material. This substrate was then temperature-equilibrated with 50 °C ethanol in the QCM-D apparatus and data logging commenced after thermal equilibrium was reached (Figure 8). The experimental temperature may induce protein denaturation, but such conditions are required for the deprotective hydrazine-treatment step and to ensure that oxime ligation occurs over a timescale shorter than response drift from the QCM-D.

Upon the addition of hydrazine monohydrate (▼, Figure 8) the QCM-D showed an immediate decrease in Δf and a concomitant rise in Δd that is attributable to the change in solution viscosity.[63] The subsequent gradual increase in Δf is evidence of a decrease in the mass on the surface of the chip; this is attributed to hydrazine-deprotection of the phthalimide stripping multilayers from the electrode surface (Scheme 3).[63-64] The dissipation value, d, is strongly influenced by not only the viscoelasticity of the adlayer but also by the density and viscosity of the bulk fluid above the film,[65] which complicates analysis of this region of the trace.

At approximately 18.5 min, the hydrazine ethanol solution was replaced with a 1 μM hydrazine aqueous solution, and at approximately 23.5 min this solution was exchanged with pH 4.5 buffer (Figure 8). Due to concerns regarding reaction of the hydrazine-treated surface with trace

contaminant aldehyde and ketone species, a 35 μM solution of horseradish peroxidase was added at approximately 25 min (▽, Figure 8), which was before full thermal equilibrium was reached. Enzyme ligation to the surface can be inferred from the steady drop in Δf between 28 and 40 min (Figure 8, inset), which is indicative of an increased adsorbed mass on the QCM sensor;[64, 66] the concomitant increases in Δd, is also attributed to formation of a protein film.[64, 66] Using the equation $\Delta m = C\Delta f$, where $C = -17.8$ ng cm^{-2} Hz^{-1} for this system,[63] we estimate the mass change, Δm, to be 2 μg cm^{-2} during protein ligation; this equates to a coverage of 50 pmol cm^{-2}.

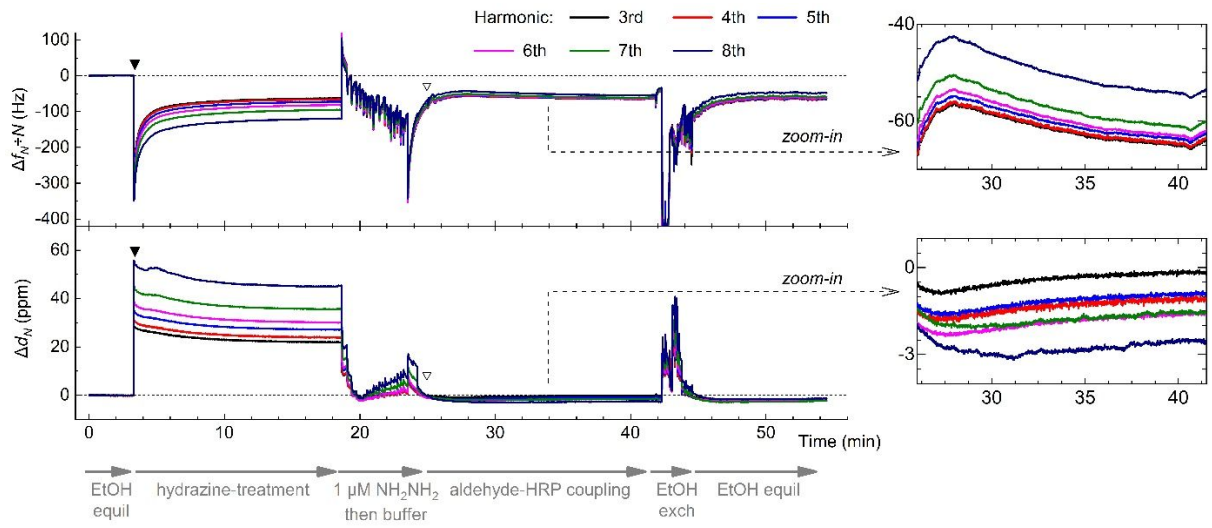

Figure 8. QCM-D results of frequency change (Δf) and dissipation change (Δd) against time for a gold-coated quartz crystal microbalance sensor electro-grafted with 2 prior to the start of the experiment. Subsequent treatments are as indicated above the plot. The experiment was conducted at 50 °C. Values for Δf are divided by the harmonic number (Q-sense convention).

SUMMARY AND CONCLUSIONS

The concept of generating a monolayer of amine functionalities on a surface via the electroreduction and subsequent deprotection of protected-amine containing diazonium salts has inspired us to harness protecting group chemistry to generate surfaces modified with a near-

monolayer of hydroxylamine. We demonstrate the utility of such surfaces for immobilizing aldehyde-containing molecules by making electrochemical measurements on surface-immobilized hydroquinone and horseradish peroxidase, with immobilization of target aldehyde species being achieved at dilute aldehyde concentrations (50 μM) and mild pH. We hope that this methodology will find a broad range of applications. The ability to functionalize semi-conducting and conducting substrates with hydroxylamine near-monolayers should be useful in stabilizing small molecule catalysts in photochemistry and solar fuel applications.[67] The immobilization of glycosylated enzymes, such as HRP, onto solid scaffolds can be utilized in the development of continuous flow biocatalysts reactors;[7] and hydroxylamine-decorated nanoparticles have already shown promise as drug delivery vehicles.[68] It is of note that although they were not required here, simple organic molecules have been identified that act as oxime reaction catalysts, speeding up the rate of reaction and permitting protein aldehyde-to-hydroxylamine ligation at neutral pH.[69] Thus, the presented methodology can be developed for immobilizing proteins or enzymes which are less robust than horseradish peroxidase.

ASSOCIATED CONTENT

Supporting Information.

Synthesis methodology; buffer solution preparation; electrochemical impedance spectroscopy methods and results; 2,5-dihydroxybenzaldehyde surface coverage experiments and analysis methodology; quinone control experiments; solution ligation experiments and product analysis; atomic force microscopy on gold; solution ferricyanide voltammetry at modified boron-doped diamond electrodes; electro-grafting of gold surfaces for XPS; control electrochemical

horseradish peroxidase experiments; electro-grafting for QCM-D; RScript code for cyclic voltammetry analysis.

AUTHOR INFORMATION

Corresponding Author

*E-mail martin.fascione@york.ac.uk, alison.parkin@york.ac.uk.

Author Contributions

All synthesis, characterization and cyclic voltammetry experiments were designed by AParkin, MAF and NDY and conducted by NDY with assistance from JD-F. EIS data was collected and analyzed by MRD. QCM-D experiments were conducted and analyzed by CFB with assistance from NDY. XPS experiments were conducted by PB with assistance from NDY and data was analyzed by AParkin with assistance from APratt and PB. The manuscript was written through contributions of all authors. All authors have given approval to the final version of the manuscript.

ACKNOWLEDGMENTS

Abigail Mortimer (UoY) is thanked for skillful construction of the electrochemical glassware. Dr S P Tear (UoY) is thanked for help in making the AFM measurements. Prof. Gideon Davies (UoY) is also gratefully acknowledged for valuable scientific discussions. This work was supported by the Biotechnology and Biological Sciences Research Council (BBSRC, studentship BB/M011151/1 to NDJY).

REFERENCES

1. Spicer, C. D.; Davis, B. G., Selective chemical protein modification. *Nat. Commun.* **2014,** *5*, 4740.

2. Boutureira, O.; Bernardes, G. J. L., Advances in Chemical Protein Modification. *Chem. Rev.* **2015,** *115* (5), 2174-2195.
3. Zhang, Y.; Park, K.-Y.; Suazo, K. F.; Distefano, M. D., Recent progress in enzymatic protein labelling techniques and their applications. *Chem. Soc. Rev.* **2018,** *47* (24), 9106-9136.
4. Meldal, M.; Schoffelen, S., Recent advances in covalent, site-specific protein immobilization. *F1000Res.* **2016,** *5* (2303).
5. Yates, N. D. J.; Fascione, M. A.; Parkin, A., Methodologies for "Wiring" Redox Proteins/Enzymes to Electrode Surfaces. *Chem. - Eur. J.* **2018,** *24* (47), 12164-12182.
6. Algar, W. R.; Dawson, P.; Medintz, I. L., *Chemoselective and Bioorthogonal Ligation Reactions: Concepts and Applications*. Wiley: 2017.
7. Britton, J.; Majumdar, S.; Weiss, G. A., Continuous flow biocatalysis. *Chem. Soc. Rev.* **2018,** *47* (15), 5891-5918.
8. Nicolini, J. V.; Ferraz, H. C.; de Resende, N. S., Immobilization of horseradish peroxidase on titanate nanowires for biosensing application. *J. Appl. Electrochem.* **2016,** *46* (1), 17-25.
9. Polsky, R.; Harper, J. C.; Dirk, S. M.; Arango, D. C.; Wheeler, D. R.; Brozik, S. M., Diazonium-Functionalized Horseradish Peroxidase Immobilized via Addressable Electrodeposition: Direct Electron Transfer and Electrochemical Detection. *Langmuir* **2007,** *23* (2), 364-366.
10. Agten, S. M.; Dawson, P. E.; Hackeng, T. M., Oxime conjugation in protein chemistry: from carbonyl incorporation to nucleophilic catalysis. *J. Pept. Sci.* **2016,** *22* (5), 271-279.
11. Arslan, M.; Tasdelen, M. A., Click Chemistry in Macromolecular Design: Complex Architectures from Functional Polymers. *Chemistry Africa* **2019,** *2* (2), 195-214.
12. Appel, M. J.; Bertozzi, C. R., Formylglycine, a post-translationally generated residue with unique catalytic capabilities and biotechnology applications. *ACS Chem. Biol.* **2015,** *10* (1), 72–84.
13. Brabham, R. L.; Spears, R. J.; Walton, J.; Tyagi, S.; Lemke, E. A.; Fascione, M. A., Palladium-unleashed proteins: gentle aldehyde decaging for site-selective protein modification. *Chem. Comm.* **2018,** *54* (12), 1501-1504.
14. Spears, R. J.; Fascione, M. A., Site-selective incorporation and ligation of protein aldehydes. *Org. Biomol. Chem.* **2016,** *14* (32), 7622-7638.
15. Ali, A. A.; Hasan, M. A.; Zaki, M. I., Dawsonite-Type Precursors for Catalytic Al, Cr, and Fe Oxides: Synthesis and Characterization. *Chemistry of Materials* **2005,** *17* (26), 6797-6804.
16. Wisdom, G. B., Horseradish Peroxidase Labeling of Antibody Using Periodate Oxidation. In *The Protein Protocols Handbook*, Walker, J. M., Ed. Humana Press: Totowa, NJ, 1996; pp 273-274.
17. Baker, M. R.; Tabb, D. L.; Ching, T.; Zimmerman, L. J.; Sakharov, I. Y.; Li, Q. X., Site-Specific N-Glycosylation Characterization of Windmill Palm Tree Peroxidase Using Novel Tools for Analysis of Plant Glycopeptide Mass Spectrometry Data. *J. Proteome Res.* **2016,** *15* (6), 2026-2038.
18. Capone, S.; Pletzenauer, R.; Maresch, D.; Metzger, K.; Altmann, F.; Herwig, C.; Spadiut, O., Glyco-variant library of the versatile enzyme horseradish peroxidase. *Glycobiology* **2014,** *24* (9), 852-863.
19. Brabham, R.; Fascione, M. A., Pyrrolysine Amber Stop-Codon Suppression: Development and Applications. *ChemBioChem* **2017,** *18* (20), 1973-1983.

20. Christman, K. L.; Broyer, R. M.; Tolstyka, Z. P.; Maynard, H. D., Site-specific protein immobilization through N-terminal oxime linkages. *J. Mater. Chem.* **2007,** *17* (19), 2021-2021.
21. Park, S.; Yousaf, M. N., An Interfacial Oxime Reaction To Immobilize Ligands and Cells in Patterns and Gradients to Photoactive Surfaces. *Langmuir* **2008,** *24* (12), 6201-6207.
22. Gooding, J. J.; Ciampi, S., The molecular level modification of surfaces: from self-assembled monolayers to complex molecular assemblies. *Chem. Soc. Rev.* **2011,** *40* (5), 2704-2718.
23. Mahouche-Chergui, S.; Gam-Derouich, S.; Mangeney, C.; Chehimi, M. M., Aryl diazonium salts: a new class of coupling agents for bonding polymers, biomacromolecules and nanoparticles to surfaces. *Chem. Soc. Rev.* **2011,** *40* (7), 4143-4166.
24. Chehimi, M. M., *Aryl Diazonium Salts: New Coupling Agents in Polymer and Surface Science*. Wiley-VCH Verlag GmbH & Co: 2012.
25. Wang, J.; Carlisle, J. A., Covalent immobilization of glucose oxidase on conducting ultrananocrystalline diamond thin films. *Diam. Relat. Mater.* **2006,** *15* (2), 279-284.
26. Zhang, X.; Tretjakov, A.; Hovestaedt, M.; Sun, G.; Syritski, V.; Reut, J.; Volkmer, R.; Hinrichs, K.; Rappich, J., Electrochemical functionalization of gold and silicon surfaces by a maleimide group as a biosensor for immunological application. *Acta Biomater.* **2013,** *9* (3), 5838-5844.
27. Gam-Derouich, S.; Lamouri, A.; Redeuilh, C.; Decorse, P.; Maurel, F.; Carbonnier, B.; Beyazıt, S.; Yilmaz, G.; Yagci, Y.; Chehimi, M. M., Diazonium Salt-Derived 4-(Dimethylamino)phenyl Groups as Hydrogen Donors in Surface-Confined Radical Photopolymerization for Bioactive Poly(2-hydroxyethyl methacrylate) Grafts. *Langmuir* **2012,** *28* (21), 8035-8045.
28. Salmi, Z.; Lamouri, A.; Decorse, P.; Jouini, M.; Boussadi, A.; Achard, J.; Gicquel, A.; Mahouche-Chergui, S.; Carbonnier, B.; Chehimi, M. M., Grafting polymer–protein bioconjugate to boron-doped diamond using aryl diazonium coupling agents. *Diam. Relat. Mater.* **2013,** *40*, 60-68.
29. Uetsuka, H.; Shin, D.; Tokuda, N.; Saeki, K.; Nebel, C. E., Electrochemical Grafting of Boron-Doped Single-Crystalline Chemical Vapor Deposition Diamond with Nitrophenyl Molecules. *Langmuir* **2007,** *23* (6), 3466-3472.
30. Juan-Colás, J.; Parkin, A.; Dunn, K. E.; Scullion, M. G.; Krauss, T. F.; Johnson, S. D., The electrophotonic silicon biosensor. *Nat. Commun.* **2016,** *7*, 12769.
31. Flavel, B. S.; Gross, A. J.; Garrett, D. J.; Nock, V.; Downard, A. J., A simple approach to patterned protein immobilization on silicon via electrografting from diazonium salt solutions. *ACS Appl. Mater. Interfaces* **2010,** *2* (4), 1184-1190.
32. Brooksby, P. A.; Downard, A. J., Electrochemical and Atomic Force Microscopy Study of Carbon Surface Modification via Diazonium Reduction in Aqueous and Acetonitrile Solutions. *Langmuir* **2004,** *20* (12), 5038-5045.
33. Page, C. C.; Moser, C. C.; Chen, X.; Dutton, P. L., Natural engineering principles of electron tunnelling in biological oxidation–reduction. *Nature* **1999,** *402* (6757), 47-52.
34. Combellas, C.; Kanoufi, F.; Pinson, J.; Podvorica, F. I., Sterically Hindered Diazonium Salts for the Grafting of a Monolayer on Metals. *J. Am. Chem. Soc.* **2008,** *130* (27), 8576-8577.
35. Mattiuzzi, A.; Jabin, I.; Mangeney, C.; Roux, C.; Reinaud, O.; Santos, L.; Bergamini, J.-F.; Hapiot, P.; Lagrost, C., Electrografting of calix[4]arenediazonium salts to form versatile robust platforms for spatially controlled surface functionalization. *Nature Communications* **2012,** *3* (1), 1130.

36. Menanteau, T.; Levillain, E.; Breton, T., Electrografting via Diazonium Chemistry: From Multilayer to Monolayer Using Radical Scavenger. *Chem. Mater.* **2013,** *25* (14), 2905-2909.
37. Lo, M.; Pires, R.; Diaw, K.; Diariatou, G.-S.; Oturan, M. A.; Aaron, J.-J.; Chehimi, M. M., Diazonium Salts: Versatile Molecular Glues for Sticking Conductive Polymers to Flexible Electrodes. *Surfaces* **2018,** *1*, 43-58.
38. Lo, M.; Diaw, A. K. D.; Gningue-Sall, D.; Aaron, J.-J.; Oturan, M. A.; Chehimi, M. M., The role of diazonium interface chemistry in the design of high performance polypyrrole-coated flexible ITO sensing electrodes. *Electrochem. commun.* **2017,** *77*, 14-18.
39. Hauquier, F.; Debou, N.; Palacin, S.; Jousselme, B., Amino functionalized thin films prepared from Gabriel synthesis applied on electrografted diazonium salts. *J. Electroanal. Chem.* **2012,** *677–680*, 127-132.
40. Lee, L.; Leroux, Y. R.; Hapiot, P.; Downard, A. J., Amine-terminated monolayers on carbon: Preparation, characterization, and coupling reactions. *Langmuir* **2015,** *31* (18), 5071-5077.
41. Malmos, K.; Dong, M.; Pillai, S.; Kingshott, P.; Besenbacher, F.; Pedersen, S. U.; Daasbjerg, K., Using a Hydrazone-Protected Benzenediazonium Salt to Introduce a Near-Monolayer of Benzaldehyde on Glassy Carbon Surfaces. *J. Am. Chem. Soc.* **2009,** *131* (13), 4928-4936.
42. Nielsen, L. T.; Vase, K. H.; Dong, M.; Besenbacher, F.; Pedersen, S. U.; Daasbjerg, K., Electrochemical Approach for Constructing a Monolayer of Thiophenolates from Grafted Multilayers of Diaryl Disulfides. *J. Am. Chem. Soc.* **2007,** *129* (7), 1888-1889.
43. Leroux, Y. R.; Fei, H.; Noël, J.-M.; Roux, C.; Hapiot, P., Efficient Covalent Modification of a Carbon Surface: Use of a Silyl Protecting Group To Form an Active Monolayer. *Journal of the American Chemical Society* **2010,** *132* (40), 14039-14041.
44. Hudson, J. L.; Jian, H.; Leonard, A. D.; Stephenson, J. J.; Tour, J. M., Triazenes as a stable diazonium source for use in functionalizing carbon nanotubes in aqueous suspensions. *Chem. Mater.* **2006,** *18* (11), 2766-2770.
45. Kongsfelt, M.; Vinther, J.; Malmos, K.; Ceccato, M.; Torbensen, K.; Knudsen, C. S.; Gothelf, K. V.; Pedersen, S. U.; Daasbjerg, K., Combining Aryltriazenes and Electrogenerated Acids To Create Well-Defined Aryl-Tethered Films and Patterns on Surfaces. *J. Am. Chem. Soc.* **2011,** *133* (11), 3788-3791.
46. Hansen, M. N.; Farjami, E.; Kristiansen, M.; Clima, L.; Pedersen, S. U.; Daasbjerg, K.; Ferapontova, E. E.; Gothelf, K. V., Synthesis and Application of a Triazene−Ferrocene Modifier for Immobilization and Characterization of Oligonucleotides at Electrodes. *J. Org. Chem.* **2010,** *75* (8), 2474-2481.
47. O'Reilly, J. E., Oxidation-reduction potential of the ferro-ferricyanide system in buffer solutions. *Biochim Biophys Acta Bioenerg* **1973,** *292* (3), 509-515.
48. Delincée, H.; Radola, B. J., Fractionation of Horseradish Peroxidase by Preparative Isoelectric Focusing, Gel Chromatography and Ion-Exchange Chromatography. *Eur. J. Biochem.* **1975,** *52* (2), 321-330.
49. Bélanger, D.; Pinson, J., Electrografting: a powerful method for surface modification. *Chem. Soc. Rev.* **2011,** *40* (7), 3995-4048.
50. Liu, G.; Liu, J.; Böcking, T.; Eggers, P. K.; Gooding, J. J., The modification of glassy carbon and gold electrodes with aryl diazonium salt: The impact of the electrode materials on the rate of heterogeneous electron transfer. *Chem. Phys.* **2005,** *319* (1-3), 136-146.

51. Petrangolini, P.; Alessandrini, A.; Berti, L.; Facci, P., An electrochemical scanning tunneling microscopy study of 2-(6-mercaptoalkyl)hydroquinone molecules on Au(111). *J. Am. Chem. Soc.* **2010,** *132* (21), 7445–7453.
52. Trammell, S. A.; Lowy, D. A.; Seferos, D. S.; Moore, M.; Bazan, G. C.; Lebedev, N., Heterogeneous electron transfer of quinone–hydroquinone in alkaline solutions at gold electrode surfaces: Comparison of saturated and unsaturated bridges. *J. Electroanal. Chem.* **2007,** *606* (1), 33-38.
53. Tse, E. C.; Barile, C. J.; Li, Y.; Zimmerman, S. C.; Hosseini, A.; Gewirth, A. A., Proton transfer dynamics dictate quinone speciation at lipid-modified electrodes. *Phys. Chem. Chem. Phys.* **2017,** *19* (10), 7086-7093.
54. Heering, H. A.; Weiner, J. H.; Armstrong, F. A., Direct Detection and Measurement of Electron Relays in a Multicentered Enzyme: Voltammetry of Electrode-Surface Films of *E. coli* Fumarate Reductase, an Iron−Sulfur Flavoprotein. *J. Am. Chem. Soc.* **1997,** *119* (48), 11628-11638.
55. Mooste, M.; Kibena-Põldsepp, E.; Marandi, M.; Matisen, L.; Sammelselg, V.; Tammeveski, K., Electrochemical properties of gold and glassy carbon electrodes electrografted with an anthraquinone diazonium compound using the rotating disc electrode method. *RSC Advances* **2016,** *6* (47), 40982-40990.
56. Kullapere, M.; Marandi, M.; Matisen, L.; Mirkhalaf, F.; Carvalho, A. E.; Maia, G.; Sammelselg, V.; Tammeveski, K., Blocking properties of gold electrodes modified with 4-nitrophenyl and 4-decylphenyl groups. *Journal of Solid State Electrochemistry* **2012,** *16* (2), 569-578.
57. Cline, K. K.; Baxter, L.; Lockwood, D.; Saylor, R.; Stalzer, A., Nonaqueous synthesis and reduction of diazonium ions (without isolation) to modify glassy carbon electrodes using mild electrografting conditions. *Journal of Electroanalytical Chemistry* **2009,** *633* (2), 283-290.
58. Lee, L.; Brooksby, P. A.; Hapiot, P.; Downard, A. J., Electrografting of 4-Nitrobenzenediazonium Ion at Carbon Electrodes: Catalyzed and Uncatalyzed Reduction Processes. *Langmuir* **2016,** *32* (2), 468-476.
59. Yeap, W. S.; Murib, M. S.; Cuypers, W.; Liu, X.; van Grinsven, B.; Ameloot, M.; Fahlman, M.; Wagner, P.; Maes, W.; Haenen, K., Boron-Doped Diamond Functionalization by an Electrografting/Alkyne–Azide Click Chemistry Sequence. *ChemElectroChem* **2014,** *1* (7), 1145-1154.
60. Kondo, T.; Hoshi, H.; Honda, K.; Einaga, Y.; Fujishima, A.; Kawai, T., Photochemical Modification of a Boron-doped Diamond Electrode Surface with Vinylferrocene. *J. Phys. Chem. C* **2008,** *112* (31), 11887-11892.
61. Beamson, G.; Briggs, D., *High Resolution XPS of Organic Polymers : The Scienta ESCA300 Database*. John Wiley and Sons Ltd: Chichester, 1992.
62. Gengenbach, T. R.; Chatelier, R. C.; Griesser, H. J., Correlation of the Nitrogen 1s and Oxygen 1s XPS Binding Energies with Compositional Changes During Oxidation of Ethylene Diamine Plasma Polymers. *Surf. Interface Anal.* **1996,** *24* (9), 611-619.
63. Singh, K.; Blanford, C. F., Electrochemical Quartz Crystal Microbalance with Dissipation Monitoring: A Technique to Optimize Enzyme Use in Bioelectrocatalysis. *ChemCatChem* **2014,** *6* (4), 921-929.
64. McArdle, T.; McNamara, T. P.; Fei, F.; Singh, K.; Blanford, C. F., Optimizing the Mass-Specific Activity of Bilirubin Oxidase Adlayers through Combined Electrochemical Quartz

Crystal Microbalance and Dual Polarization Interferometry Analyses. *ACS Appl. Mater. Interfaces* **2015,** *7* (45), 25270-25280.
65. McNamara, T. P.; Blanford, C. F., A sensitivity metric and software to guide the analysis of soft films measured by a quartz crystal microbalance. *Analyst* **2016,** *141* (10), 2911-2919.
66. Nelson, G. W.; Parker, E. M.; Singh, K.; Blanford, C. F.; Moloney, M. G.; Foord, J. S., Surface Characterization and in situ Protein Adsorption Studies on Carbene-Modified Polymers. *Langmuir* **2015,** *31* (40), 11086-11096.
67. Zhang, B.; Sun, L., Artificial photosynthesis: opportunities and challenges of molecular catalysts. *Chem. Soc. Rev.* **2019,** *48* (7), 2216-2264.
68. Ferris, D. P.; McGonigal, P. R.; Witus, L. S.; Kawaji, T.; Algaradah, M. M.; Alnajadah, A. R.; Nassar, M. S.; Stoddart, J. F., Oxime Ligation on the Surface of Mesoporous Silica Nanoparticles. *Org. Lett.* **2015,** *17* (9), 2146-2149.
69. Larsen, D.; Kietrys, A. M.; Clark, S. A.; Park, H. S.; Ekebergh, A.; Kool, E. T., Exceptionally rapid oxime and hydrazone formation promoted by catalytic amine buffers with low toxicity. *Chem Sci* **2018,** *9* (23), 5252-5259.

Table of Contents Graphic